Magnetic Wheel Optimization for Undercarriage of Self-Acting Robot

Vladimír Kindl[*], Roman Pechánek[*], Antonín Předota[*]

[*]Faculty of Electrical Engineering, University of West Bohemia in Pilsen, Univerzitní 8, Pilsen,
The Czech Republic, e-mail: vkindl@kev.zcu.cz, rpechane@kev.zcu.cz, apredota@kte.zcu.cz

Abstract **This paper deals with the dimensional and the material optimization of the robot magnetic wheel. A maximum value of the attracting force and the reduction of the weight are demanded. Three calculation techniques were used. The analytical solution shows conversion of the real wheel gap to a fictional constant gap and allows getting the total attracting force under some simplification. A numerical linear model respects dimension of the wheel exactly. Results are comparable with the precious technique. The last one technique is based on a non-linear model. It extends the linear model by accurate characteristics of the steel.**

Keywords **dimensional optimization, robot undercarriage, attracting force, non-linear model.**

I. INTRODUCTION

The most important function of the robot undercarriage is to ensure the adhesion with the understructure. In case of the iron understructure the undercarriage can be made from a magnetic material and the robot is able to move upside down. The undercarriage consists from wheels and a permanent magnet.

The undercarriage can be optimized to achieve an effective geometrical design with regard to the magnetic circuit. The maximum value of the attractive force has to be fined out.

The permanent magnet should to be chosen with regard to the maximum magnetic field intensity. The maximum value of the NdFeB magnetic field intensity is approximately $H_C = -830$ kA/m. This material was used in the practical design. The magnetic material strongly depends on the temperature [1] and this influence has to be considered in the calculation.

II. MAGNETIC CIRCUIT DESIGN

The first optimization was done for the ideal iron ($\mu_R = \infty$) because a low value of magnetic flux density is supposed. The magnetic circuit is not fed by a current source. Only the permanent magnet is used. The next optimization presumption in this first optimization is the same magnetic flux in the permanent magnet and in the air gap. The dispersion is not considered. Eq. (1) presents a mathematical expression of the permanent magnet operating value assessment.

$$B_M = -\mu_0 \frac{S_\delta}{S_M} \frac{l_M}{\delta} H_M \tag{1}$$

Eq. (1) can be used only for the basic calculations. In fact the situation is more complicated. The accurate calculation can be done by conversion of the real gap to a fictional gap with constant value [2] which much more corresponds to the real gap and represents the reality more accurately. The magnetic field intensity describes eq. (2).

$$H(x) = \frac{U_M}{\delta + r\left[1 - \cos\left(arc\sin\left(\frac{x}{r}\right)\right)\right]} \tag{2}$$

This value is falling down very quickly back of the wheel contact. The borderline of the relevant magnetic field intensity was determined from dependence of the magnetic field intensity to the wheel contact distance. The situation is depicted in fig. 1.
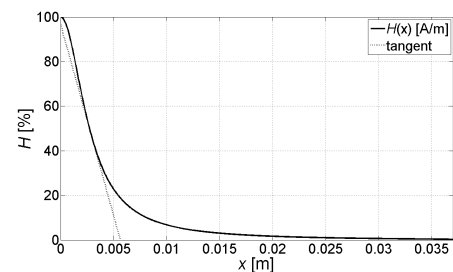

Fig. 1. Magnetic field intensity in the air gap

The relevant magnetic field intensity is from the contact to $x_{MAX} = 5.4$ mm. In the next calculation only the magnetic field intensity since $x = 0$ to $x = 5.4$ mm is considered.

Knowledge of the relevant magnetic field intensity allows determining the fictional gap. The value can by calculated according to eq. (3).

$$l_{EKV} = \frac{1}{x_{MAX}} \int_0^{x_{MAX}} \left(\delta + r\left[1 - \cos\left(arc\sin\left(\frac{x}{r}\right)\right)\right] \right) dx \tag{3}$$
$$= 0.24 \; mm$$

This value is essential to calculate eq. (1). The operating value was determined $H_b = 66520$ A/m, $B_b = 0.96$ T. It means $\Phi = B_b S_M = 0.603$ mWb.

With regard to the saturation the surface area of one tooth is $S_Z = 40.2$ mm^2. The tooth thickness was appointed $b_Z = 9$ mm with regard to $B_{KRIT} = 1.5$ T. The wheel is shown in fig. 2.
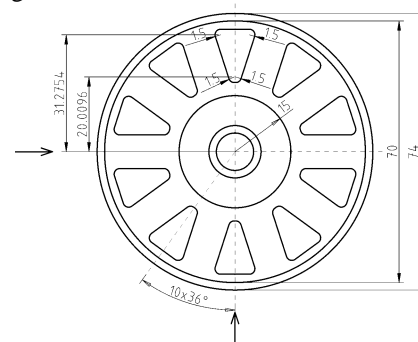

Fig. 2. Wheel with grooves

III. FORCE SPECIFICATION

a) Analytically

This technique was completed under some simplifications of the problem. Only a basic magnetic circuit is considered. The source of the magnetic voltage is loaded by two serial reluctances which represents the fictive air gap. The voltage of both reluctances is the same, the calculation can be done only for one of them and the result multiplied by two.

The energy in the magnetic circuit is mostly in the air gap. Eq. (4) expresses the force in the gap.

$$F = -\frac{dW_M}{dx} = -\frac{1}{2}\mu_0 H^2 S_\delta \qquad (4)$$

The total force of the undercarriage attracting force is $F_{TOT} = 140$ N. The robot must weigh less than 14 kg.

b) Numerically – linear model

The static problem is considered. The attracting force changes slightly its value during the wheel motion. This inaccuracy is supposed not more than 5%. This value is not significant for the design. The linear model respects the real shape of the air gap, the leakage flux and the demagnetization of the permanent magnet.

With regard to the real operation environment the additional constant gap is considered 0.1 mm. This value is sufficient for the effective undercarriage design. The next fig. 3 presents the FEM model.
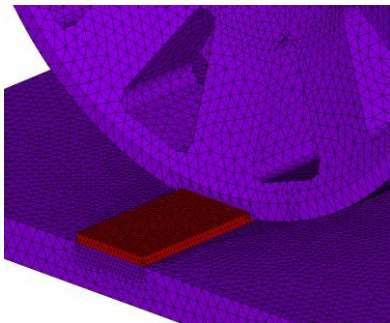

Fig. 3. FEM detailed model

The model respects the demagnetization of the permanent magnet. The difference between analytical and numerical solution can by expressed by the total value of the force. It shows eq. (5).

$$\delta = \frac{F_{analyt.}}{F_{numer.}} = \frac{177}{170} = 4.1\% \rightarrow 17\,\text{N} \qquad (5)$$

This conclusion permits to accept the 3D numerical model and make improvement of its parameters.

c) Numerically – non-liner model

This model extends the previous model by a non-zero magnetic iron reluctance and is closer to the physical reality. The considered material is steel 11 373.1.

The difference between the linear and the non-linear model is expressed by eq. (6).

$$\delta = \frac{F_{linear}}{F_{non-liner}} = \frac{170}{118} = 44\% \rightarrow 110\,\text{N} \qquad (6)$$

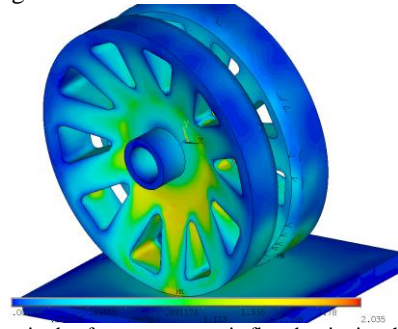The result of the non-liner numerical model is presented in fig. 4.

Fig. 4. Magnitude of vectors magnetic flux density in wheel

The difference is mostly given by two factors. The first is drop of the magnetic voltage in the steel and the second is the saturation caused by the skid between the wheel and the understructure.

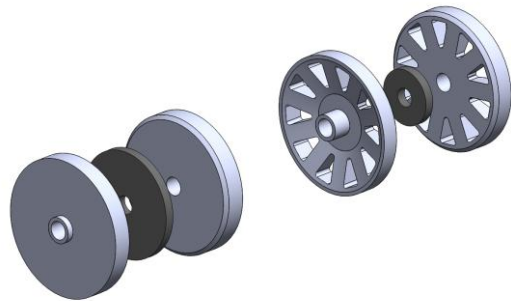The basic and the new undercarriage are shown in fig. 5.

Fig. 5. Basic and new undercarriage

IV. CONCLUSION

The design unequivocally indicates that the basic solution of the robot undercarriage can be optimized. Wheels were unnecessarily voluminous and it causes a worthless weight. Three techniques were used for results calculation. All of them are in a good agreement and allows declaring a correct design solution. The new undercarriage design fully respects the magnetic circuit and the undesirable saturation. Wheels design should forthwith follow two essential parameters. The shaft cannot consist from a magnetic material. It would cause an unacceptable magnetic circuit. The second demand on wheels is to turn one wheel by 18°. It guarantees reduction of the pulse robot motion.

V. ACKNOWLEDGEMENTS

VI. REFERENCES

[1] Xiao J., Sadegh A., Elliot M., Calle A., Persad A., Chiu H. M.: "Design of Mobile Robots with Wall Climbing Capability", Proc. of the 2005 IEEE/ASME Int. Conf. on Advanced Intelligent Mechatronics, pp438-443, July 24-28, 2005.

[2] Kopylov, I. P. et al.: Stavba elektrických strojů (Design of electric machinery). SNTL, Praha, 1988. ISBN 04-532-88

[3] Fischer, W.; Caprari, G.; Siegwart, R.; Moser, R.; "Compact magnetic wheeled robot for inspecting complex shaped structures in generator housings and similar environments," Intelligent Robots and Systems, 2009. IROS 2009. IEEE/RSJ International Conference on , vol., no., pp.4116-4121, 10-15 Oct. 2009